RibBX of Bradyrhizobium ORS285 Plays an Important Role in Intracellular Persistence in Various Aeschynomene Host Plants

Nico Nouwen, Jean-Francois Arrighi, Djamel Gully, Eric Giraud

MPMI Vol. 34, No. 1, 2021, pp. 88–99. https://doi.org/10.1094/MPMI-07-20-0209-R

e-Xtra*

RibBX of *Bradyrhizobium* ORS285 Plays an Important Role in Intracellular Persistence in Various *Aeschynomene* Host Plants

Nico Nouwen,† Jean-Francois Arrighi, Djamel Gully, and Eric Giraud

Laboratoire des Symbioses Tropicales et Méditerranéennes, IRD, CIRAD, SupAgro, INRAE, University of Montpellier, Montpellier, France

Accepted 23 September 2020.

Bradyrhizobium ORS285 forms a nitrogen-fixating symbiosis with both Nod factor (NF)-dependent and NF-independent *Aeschynomene* spp. The *Bradyrhizobium* ORS285 *ribBA* gene encodes for a putative bifunctional enzyme with 3,4-dihydroxybutanone phosphate (3,4-DHBP) synthase and guanosine triphosphate (GTP) cyclohydrolase II activities, catalyzing the initial steps in the riboflavin biosynthesis pathway. In this study, we show that inactivating the *ribBA* gene does not cause riboflavin auxotrophy under free-living conditions and that, as shown for RibBAs from other bacteria, the GTP cyclohydrolase II domain has no enzymatic activity. For this reason, we have renamed the annotated *ribBA* as *ribBX*. Because we were unable to identify other *ribBA* or *ribA* and *ribB* homologs in the genome of *Bradyrhizobium* ORS285, we hypothesize that the ORS285 strain can use unconventional enzymes or an alternative pathway for the initial steps of riboflavin biosynthesis. Inactivating *ribBX* has a drastic impact on the interaction of *Bradyrhizobium* ORS285 with many of the tested *Aeschynomene* spp. In these *Aeschynomene* spp., the ORS285 *ribBX* mutant is able to infect the plant host cells but the intracellular infection is not maintained and the nodules senesce early. This phenotype can be complemented by reintroduction of the 3,4-DHBP synthase domain alone. Our results indicate that, in *Bradyrhizobium* ORS285, the RibBX protein is not essential for riboflavin biosynthesis under free-living conditions and we hypothesize that its activity is needed to sustain riboflavin biosynthesis under certain symbiotic conditions.

Keywords: bacteria-plant symbiosis, mutualism, nodule organogenesis, rhizobium, rhizobium-legume symbiosis, vitamin B2

Bradyrhizobium sp. ORS285 is a photosynthetic Gram-negative bacterium that belongs to the order Rhizobiales. It invades the base of lateral roots or the adventitious root primordia on the stem of host *Aeschynomene* spp. and triggers the formation of a new plant organ, the so called nodule. Within plant cells of the formed nodules, the bacteria are chronically maintained and differentiate into dinitrogen-fixing bacteroids. The ORS285–*Aeschynomene* interaction is a very interesting symbiotic model because (i) depending on the *Aeschynomene* spp., the infection and nodule organogenesis does or does not rely on the bacterial synthesis of Nod factors (NFs) (Giraud et al. 2007) and (ii) between NF-independent and NF-dependent *Aeschynomene* spp., a drastic difference in morphology of the ORS285 bacteroids is observed (i.e., the bacteroids are spherical in NF-independent species whereas they are elongated in the NF-dependent ones) (Czernic et al. 2015).

Riboflavin (vitamin B2) is the precursor of flavin mononucleotide (FMN) and flavin adenine dinucleotide (FAD). FMN and FAD are cofactors of flavoproteins that are involved in a large number of reactions concerning energy metabolism such as degradation of fatty acids, carbohydrates, and amino acids (Abbas and Sibirny 2011). Flavoproteins also mediate reactions during biosynthesis and DNA repair, bioluminescence, and light sensing (Christie et al. 2015; Dunlap 2014; Tagua et al. 2015). Moreover, flavin nucleotides play an crucial role in the synthesis of secondary metabolites and metabolism of other vitamins such as pyridoxine (vitamin B6), cobalamine (vitamin B12), and folate (Haase et al. 2014). Experiments with a riboflavin auxotroph of *Rhizobium trifolii* showed that the bioavailability of riboflavin strongly influences the symbiotic interaction with different red clover (*Trifolium pratense*) cultivars and that the effectiveness correlated with the flavin content in the nodules (Pankhurst et al. 1974; Schwinghamer 1970). Addition of riboflavin to the plant growth medium also has been shown to stimulate *Medicago sativa* root colonization by *Ensifer meliloti* (Yang et al. 2002; Yurgel et al. 2014). Bacterial flavin metabolism has also been shown to be important for the intracellular survival and mouse colonization by *Brucella abortus* (Bonomi et al. 2010). This shows that riboflavin plays an important role in symbiotic and pathogenic microbe–host interactions.

Plants and the majority of bacteria are able to synthesize riboflavin de novo through the riboflavin biosynthetic pathway. In this pathway, one molecule of guanosin-5′-triphosphate (GTP) and two molecules of ribulose-5-phosphate are converted into one molecule of riboflavin (Fig. 1A). The bacterial enzymes (*Escherichia coli* abbreviations are used for clarity) in this pathway are GTP cyclohydrolase II (RibA), 3,4-dihydroxy-2-butanone 4-phosphate (3,4-DHBP) synthase (RibB), pyrimidine deaminase/reductase (RibD), 6,7-dimethyl-8-ribityllumazine

†Corresponding author: N. Nouwen; nico.nouwen@ird.fr

Funding: This work was supported by a grant from the French National Research Agency (grant "SymEffectors"; ANR-16-CE20-0013).

*The *e*-Xtra logo stands for "electronic extra" and indicates there are supplementary materials published online.

The author(s) declare no conflict of interest.

synthase (RibH), and riboflavin synthase (RibE). The genomic organization of *rib* genes and the presence of paralogs is highly variable (García-Angulo 2017). In some bacteria, the *rib* genes are clustered whereas, in others, they are found as monocistronic elements scattered over the chromosome. Also, bacteria containing duplications or multiplications of one or more *rib* genes have been found. In addition, sometimes the GTP cyclohydrolase II and 3,4-DHBP synthase are fused and form a hybrid enzyme encoded by the *ribBA* gene, and the pyrimidine deaminase and reductase function of RibD can be encoded by two separate genes, *ribD* (deaminase) and *ribG* (reductase), respectively. Riboflavin biosynthesis has shown to be regulated by an FMN riboswitch (also called RFN element), a RNA sequence present in the 5′-untranslated region of some mRNAs encoding riboflavin biosynthesis enzymes (Winkler et al. 2002). In general, the binding of FMN to the RFN element downregulates transcription or translation of the downstream genes. For a long time, RFN element regulation has been seen as the sole mechanism to control riboflavin biosynthesis in bacteria. However, studies in the last decade have shown that other, more complex regulation mechanisms exist (Balasubramanian et al. 2010; da Silva Neto et al. 2013; Tan et al. 2015; Taniguchi and Wendisch 2015), which makes sense given the diverse role flavoproteins play in the cellular metabolism.

Scattered over the chromosome, several putative riboflavin biosynthesis genes have been found in *Bradyrhizobium* ORS285 (Fig. 1B to D). These include (i) the *ribD*, *ribE* (called *ribC* in ORS285), and *ribH*1 genes which form an operon structure (Fig. 1B); (ii) a second copy of *ribH* (*ribH2*) (Fig. 1C); and (iii) a gene annotated as *ribBA*, encoding a putative bifunctional 3,4-DHBP synthase/GTP cyclohydrolase II which forms an operon with a gene annotated as *gcdH*, encoding a putative glutaryl-CoA dehydrogenase, and likely a third gene, encoding a putative β-lactamase (*BRAD5118* = BRAD285_v2_5118) (Fig. 1D). This genomic context of *rib* genes in ORS285 is very well conserved in bradyrhizobia.

In this study, we have characterized the annotated *ribBA* gene of *Bradyrhizobium* ORS285 and its role in symbiosis with different *Aeschynomene* spp. We show that the protein encoded by *ribBA* does not have GTP cyclohydrolase II activity, as was previously shown for several other annotated *ribBA* genes (Brutinel et al. 2013). In line with these observations, we have renamed the gene *ribBX*. Interestingly, inactivation of *ribBX* did not lead to riboflavin auxotrophy under free-living conditions but had a drastic impact on the intracellular persistence of the ORS285 strain, especially in NF-independent *Aeschynomene* spp.

RESULTS

Inactivation of the *Bradyrhizobium* ORS285 *ribBA* gene does not result in riboflavin auxotrophy.

A large screen for mutations that affect the symbiosis between photosynthetic *Bradyrhizobium* ORS278 and *Aeschynomene indica* showed that a TN5 insertion into a gene annotated as *ribBA* results in the formation of nodules that are unable to fix nitrogen (Bonaldi et al. 2010). Based on homology, the *ribBA* gene of *Bradyrhizobium* ORS278 is annotated to encode for a bifunctional enzyme with the activities of both 3,4-DHBP synthase (RibB) and GTP cyclohydrolase II (RibA), which catalyze two essential reactions in riboflavin biosynthesis (García-Angulo 2017). In bradyrhizobia, the genomic context of *ribBA* is very well conserved (for example, as in the genetic organization in *Bradyrhizobium* ORS285) (Fig. 1D). Given its organization, *ribBA* most probably forms an operon with the *gcdH* gene and this operon might also include a third gene encoding for a putative β-lactamase (BRAD285_v2_5118). The *gcdH* gene encodes for a glutaryl-CoA dehydrogenase, an enzyme that can play a role in many different pathways (fatty acid/lysine/benzoate degradation, tryptophan metabolism, and metabolism of secondary metabolites). Interestingly, in the reaction catalyzed by GcdH, a derivative of riboflavin, FAD, functions as cofactor by accepting the electron in the oxidation of the substrate, and its reoxidation by an electron-transfer flavoprotein completes the catalytic cycle of the enzyme. Transcribed in the opposite direction of *ribBA* is a gene that is annotated in *Bradyrhizobium* genomes as putative 2-aminoadipate transaminase or transaminase. However, closer examination of the gene product showed that, in addition to the transaminase domain, it also contains a helix-turn-helix DNA-binding domain. For this reason, we hypothesized that the gene product is not an enzyme but a transcriptional regulator belonging to the GntR family (Rigali et al. 2002) and, as such, could be implicated in the expression of the *ribBA-gcdH*(*-BRAD5118*) operon. To investigate the role of *ribBA* and the surrounding genes in the symbiotic interaction of *Bradyrhizobium* ORS285 with *Aeschynomene* legumes, we have inactivated the *ribBA*, *gcdH*, *BRAD5118*, and *gntR-like* genes by integration of the nonreplicative plasmid pJG194(*-gusA*) (Griffitts and Long 2008). All mutant strains were able to grow on solid minimal growth medium without riboflavin supplementation (Fig. 1E) and had similar growth rates compared with the wild-type (WT) strain when grown in equivalent liquid medium (Fig. 1F). This observation is remarkable because RibB and RibA are the only known

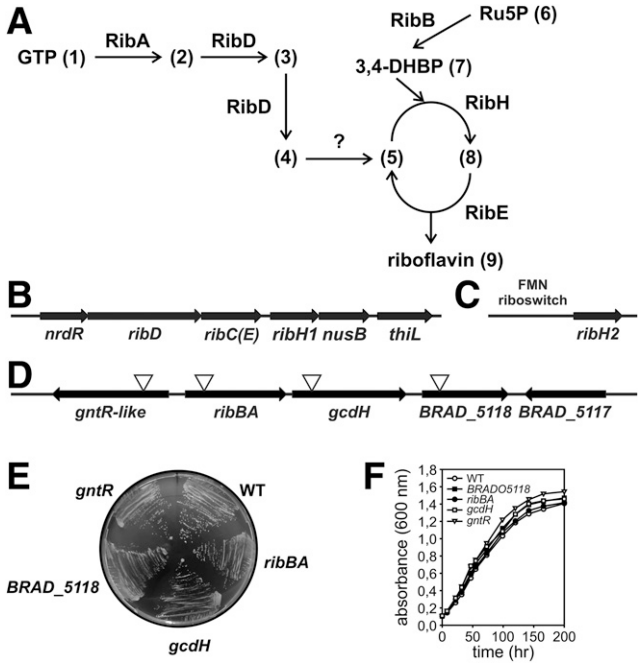

Fig. 1. A, Riboflavin biosynthesis pathway and enzymes involved in the different reactions in *Escherichia coli*: 1 = guanosine triphosphate (GTP); 2 = 2,5-diamino-5-ribosylamino-4(3H)-pyrimidone-5′-phosphate; 3 = 5-amino-6-ribosylamino-2,4(1H,3H)-pyrimidinione-5′-phosphate; 4 = 5-amino-6-ribitylamino-2,4(1H,3H)-pyrimidinione-5′-phosphate; 5 = 5-amino-6-ribitylamino-2,4(1H,3H)-pyrimidinione; 6 = ribulose-5-phosphate (Ru5P); 7 = 3,4-dihydroxy-2-butanone-4-phosphate (3,4-DHBP); 8 = 6,7-dimethyl-8-ribityllumazine; and 9 = riboflavin. **B** to **D,** Schematic representation of the different genomic regions of putative *rib* genes in *Bradyrhizobium* ORS285. The insertion of the nonreplicative plasmid to inactivate the different genes in the *ribBA* region are indicated by an arrow in D. **E,** Growth of *Bradyrhizobium* ORS285 and derivatives on minimal medium agar plates without riboflavin supplementation. **F,** Representative growth curves of *Bradyrhizobium* ORS285 and derivatives in minimal medium without riboflavin supplementation.

enzymes to catalyze the first steps of the riboflavin biosynthetic pathway and, by BLAST analysis using ORS285 *ribBA* as query and an E-value cut-off ≤1, we did not identify an additional copy of *ribBA* or putative *ribA* and *ribB* homologs in the genome of the ORS285 strain. These findings suggest that *Bradyrhizobium* ORS285 can use unconventional enzymes for the biosynthesis of riboflavin.

The GTP cyclohydrolase II domain in RibBA of *Bradyrhizobium* ORS285 cannot complement an *E. coli ribA* mutant.

Because *ribBA* is not essential for growth, one can ask whether the gene product does, indeed, have the two enzyme activities predicted from the presence of the two functional domains 3,4-DHBP synthase (PF00926) and GTP cyclohydrolase II (PF00925). This question is all the more justified given that Brutinel et al. (2013) indicated that approximately 40% of the *ribBA* genes are likely misannotated and should be renamed *ribBX*, because the encoded GTP cyclohydrolase II domain lacks catalytic activity. To obtain insight into the potential functionality of the two enzymatic domains in ORS285 RibBA, we examined the amino acid sequences and compared these with the RibB and RibA enzymes of *E. coli* because their three-dimensional structures have been solved and the amino acids that are important for enzyme activity are known (Kelly et al. 2001; Liao et al. 2001; Ren et al. 2005). ClustalW analysis showed that the active site residues of *E. coli* RibB are totally conserved in the N-terminal region of the RibBA sequence of ORS285 and supplementary analyzed RibBA homologs (Supplementary Fig. S1). In contrast, the RibBA sequences from ORS285 and other examined bradyhizobia lack the amino acids for zinc binding and ring opening that are critical for GTP cyclohydrolase II activity in *E. coli* RibA (Fig. 2A). To further investigate the functionality of ORS285 RibBA, we used *E. coli* riboflavin auxotrophs with transposon insertions in *ribA* and *ribB*. In addition to a plasmid expressing the full-length ORS285 *ribBA* gene, the two *E. coli* mutants were also transformed with plasmids that only express the N-terminal 3,4-DHBP synthase domain (RibB) or C-terminal GTP cyclohydrolase II domain (RibA). The resulting strains were grown on minimal medium agar plates without riboflavin supplementation to analyze functional complementation of riboflavin biosynthesis. Plasmids expressing the full-length *ribBA* sequence or the 3,4-DHBP synthase domain alone were able to complement the *E. coli ribB* mutant for growth in the absence of riboflavin (Fig. 2B). In contrast, none of the plasmids were able to complement the *E. coli ribA* mutant. The above data indicate that the *ribBA* gene of ORS285 does not possess GTP cyclohydrolyse II activity (Fig. 2C). For this reason, we have renamed the ORS285 *ribBA* gene *ribBX*, as was done by Brutinel et al. (2013); and, for clarity, we have abbreviated the domain with homology to RibA as "RibX domain" in the rest of this study.

RibBX is required for a symbiotic interaction with Nod factor-independent *Aeschynomene* spp.

Bradyrhizobium ORS285 has a relatively broad host range and, depending on the plant species, uses NF-independent or NF-dependent mechanisms to establish a symbiotic interaction (Giraud et al. 2007). To investigate the effect of inactivating

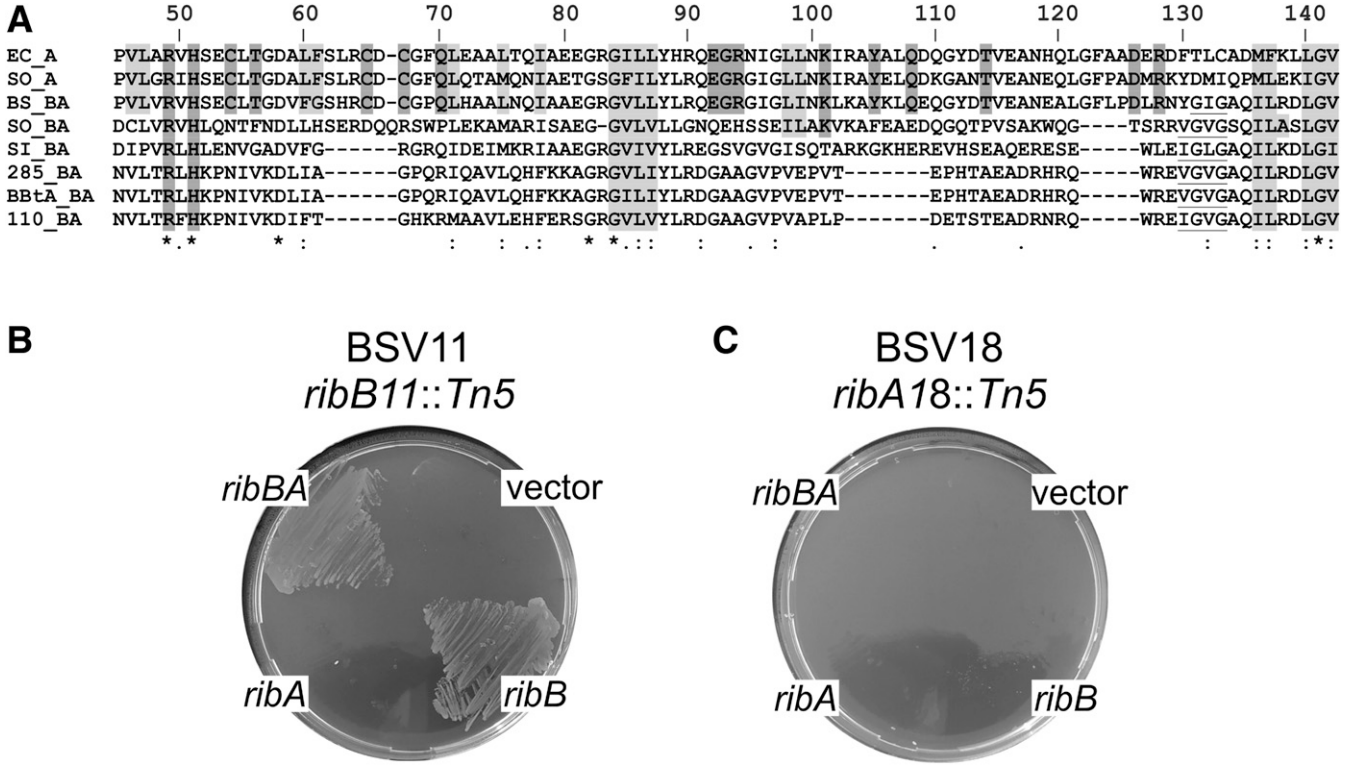

Fig. 2. A, ClustalW alignment of *Escherichia coli* RibA and guanosine triphosphate (GTP) cyclohydrolase II domains encoded by annotated *ribBA* genes of *Bradyrhizobium* ORS285 and different other bacteria. Only the region important for *E. coli* RibA functioning is shown. Residues that participate in the catalytic mechanism in *E. coli* RibA are boxed in dark gray, and nonpolar residues that form the hydrophobic core in the crystal structure are boxed in light gray. EC_A = *Escherichia coli* RibA, SO_A = *Shewanella oneidensis* MR-1 RibA, BS_BA = *Bacillus subtilus* RibBA, SO_BA = *S. oneidensis* MR-1 RibBX, SI_BA = *Ensifer meliloti* RibBA, 285_BA = *Bradyrhizobium* ORS285 RibBA, BBtA_BA = *Bradyrhizobium* BtaI1 RibBA, and 110_BA = *Bradyrhizobium diazoefficiens* USDA110 RibBA. **B,** Complementation of an *E. coli ribB* mutant by plasmids expressing *Bradyrhizobium* ORS285 RibBA, the 3,4-dihydroxybutanone phosphate (3,4-DHBP) synthase domain (RibB), and the GTP cyclohydrolase II domain (RibA), respectively. **C,** Complementation of an *E. coli ribA* mutant by plasmids expressing *Bradyrhizobium* ORS285 RibBA, the 3,4-DHBP synthase domain (RibB), and the GTP cyclohydrolase II domain (RibA), respectively.

genes in the *ribBX*-containing region on the symbiotic interaction with an NF-independent host plant, we infected our model species *A. evenia* with the WT and *ribBX*, *gcdH*, *BRAD5118*, and *gntR* mutants. At 23 days postinfection (dpi), only noninoculated plants and plants inoculated with the *ribBX* mutant showed drastic differences with plants inoculated with the WT strain. Noninoculated and *ribBX*-infected plants had clear nitrogen starvation signs such as reduced plant growth and foliar chlorosis (Fig. 3A). In addition, whereas nodules on plants infected with the WT and *gcdH*, *BRAD5118*, or *gntR* mutant strains had a pink or red color, the majority of nodules on *ribBX*-infected plants were entirely white (Fig. 3B). The white color is symptomatic for nodules that do not fix nitrogen. Analysis of the number of nodules at 23 dpi showed that plants infected with the *ribBX* mutant contained approximately twice the number of nodules compared with plants inoculated with the WT or *gcdH*, *BRAD5118*, or *gntR* mutant strains (Fig. 3C). An increase in nodule number is often found with rhizobia mutants that form nonfunctional nodules, and is accredited to a mechanism called autoregulation of nodulation that assures an equilibrium between benefits of nodule formation and energy costs for the plant (Wang et al. 2018). In line with the visual observations, the acetylene reduction assay (ARA) showed that nodules on plants infected with the *ribBX* mutant had virtual zero nitrogenase enzyme activity, and that the nitrogenase enzyme activity of nodules elicited by *gcdH*, *BRAD5118*, or *gntR* mutant strains were comparable with that of the WT (Fig. 3D). To investigate whether the absence of nitrogenase activity is a symbiotic or general phenotype of the *ribBX* mutant, we have also performed the ARA assay under free-living conditions. In the absence of riboflavin supplementation to the growth medium and conditions that induce the expression of nitrogenase genes (i.e., low oxygen tension and absence of a nitrogen source), the nitrogenase enzyme activity of the *ribBX* strain was comparable with that of the WT strain (Fig. 4A). This shows that the observed absence of nitrogenase enzyme activity in nodules is due to a disturbed symbiotic interaction of the *ribBX* mutant with the *A. evenia* host plant.

Cytological observations showed that, in contrast to nodules found on plants infected with the *gcdH* and *BRAD5118* mutant strain, the nodules induced by the *ribBX* mutant were often hollow inside and displayed no β-glucuronidase (GUS) activity (these three mutants were created by inserting a promotorless *gusA* cassette into the gene) (Fig. 4E versus G and H). However, whereas the majority of *ribBX* nodules showed no GUS activity, in some nodules on the same plant, low GUS activity was detected (Fig. 4F). These nodules were often small, suggesting that these are young, developing nodules. To analyze whether the *ribBX* gene is expressed in a WT context, we also

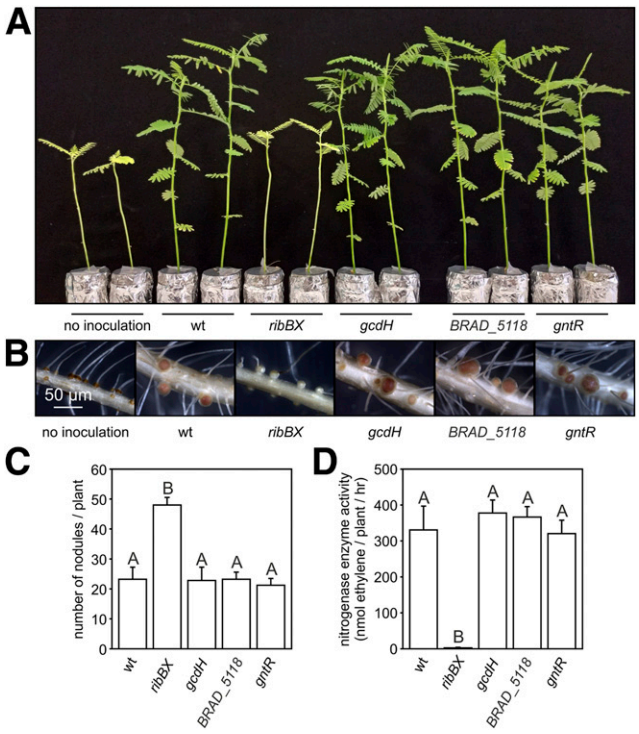

Fig. 3. ORS285 *ribBX* inactivation affects the symbiotic interaction with *Aeschynomene evenia* (CIAT22838). **A,** Comparison of the growth of *A. evenia* plants inoculated with wild-type (wt) ORS285, ORS285 *ribBX*, ORS285 *gcdH*, ORS285 *BRAD5118*, and ORS285 *gntR*. Noninoculated plants (ni) were used as control. **B,** Mature nodules on *A. evenia* plants inoculated with ORS285, ORS285 *ribBX*, ORS285 *gcdH*, ORS285 *BRAD5118*, and ORS285 *gntR*. Note the presence of white-colored nodules (black arrow) on *A. evenia* plants inoculated with the ORS285 *ribBX* strain. **C,** Number of root nodules on *A. evenia* plants inoculated with ORS285, ORS285 *ribBX*, ORS285 *gcdH*, ORS285 *BRAD5118*, and ORS285 *gntR*. The mean number of nodules per plant ($n = 5$) at 23 days postinfection (dpi) is presented. **D,** Acetylene-reducing activity of *A. evenia* plants inoculated with ORS285, ORS285 *ribBX*, ORS285 *gcdH*, ORS285 *BRAD5118*, and ORS285 *gntR* at 23 dpi. The mean amount of produced ethylene per hour and per plant ($n = 5$) is indicated. Error bars (C and D) represent standard errors of the mean and letters represent conditions with significant difference according to Tukey's test ($P < 0.05$).

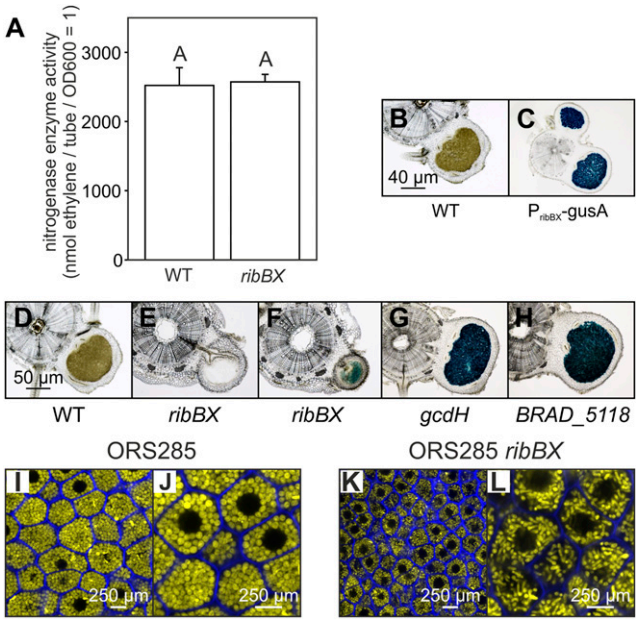

Fig. 4. A, ORS285 *ribBX* mutant has nitrogenase enzyme activity under free-living conditions. Ethylene production of wild-type (WT) ORS285 and ORS285 *ribBX* grown for 7 days in vacuette tubes containing BNM-B agar (0.8% wt/vol) medium without riboflavin supplementation and 10% acetylene gas. The mean amount of produced ethylene per tube ($n = 4$) is indicated. OD600 = optical density at 600 nm. Error bars represent standard errors of the mean and letters represent conditions with significant difference according to Tukey's test ($P < 0.05$). **B** and **C,** *RibBX* promoter activity in nodules of *Aeschynomene evenia*. *A. evenia* plants were infected with the WT or P_{ribBX}-*gusA* reporter strain and, at 15 days postinfection (dpi), the β-glucuronidase activity in 70 µM nodule sections was determined by 5-bromo-4-chloro-3-indoxyl-β-D-glucuronide cyclohexylammonium salt (X-Gluc) staining. β-Glucuronidase activity in *A. evenia* nodules induced by **D,** WT; **E** and **F,** *ribBX*; **G,** *gcdH*; and **H,** *BRAD5118* mutant strains of *Bradyrhizobium* ORS285. Nodule sections (70 µM) were stained for 30 min with X-Gluc. Confocal microscopic analysis of nodules induced by **I** and **J,** WT ORS285 and **K** and **L,** ORS285 *ribBX* mutant. ORS285 bacteriods are spherical (J) whereas the intracellular bacteria in nodules induced by the ORS285 *ribBX* mutant have an elongated shape (L).

constructed a reporter strain in which the *gusA* gene is placed under the control of the promoter region of the *ribBX* gene. This reporter strain showed that the *ribBX* gene is expressed in WT mature nodules (Fig. 4C). All of these observations suggest that the first stages of the infection and nodule organogenesis process are not affected by the *ribBX* mutation but that, at later stages, the infection cannot persist and nodules senesce prematurely. To investigate the infection process in more detail, we have transformed the ORS285 *ribBX* mutant with a plasmid that expresses superyellow fluorescent protein (sYFP) constitutively. *A. evenia* plants were infected with this sYFP-tagged strain and nodules present at 7 dpi were analyzed by confocal microscopy. This early time point of analysis was chosen to observe infection stages before nodule senescence in *ribBX*-infected plants emerged. At 7 dpi, plants infected by the WT and *ribBX* strain contained mature-sized nodules in which plant cells in the central tissue were uniformly infected by bacteria (Fig. 4I and K). However, whereas WT bacteria in these nodules are differentiated into spherical bacteroids, they have an elongated shape in RibBX nodules (Fig. 4J versus L). This indicates that, in the absence of the RibBX protein, ORS285 cells are unable to differentiate into the spherical bacteroids that are characteristic for the symbiotic interaction with NF-independent *Aeschynomene* legumes.

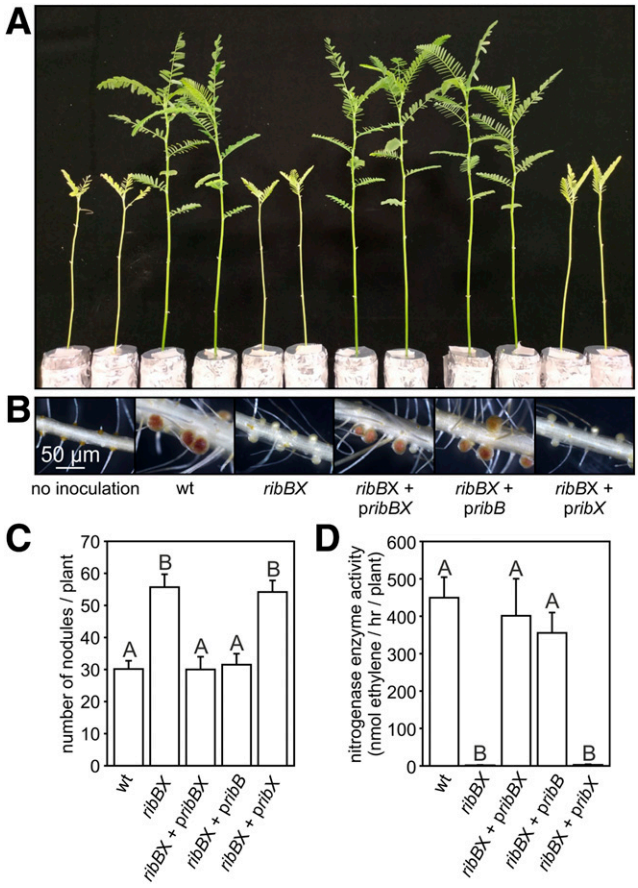

Fig. 5. Expression of the 3,4-dihydroxybutanone phosphate synthase domain complements the symbiotic phenotype of the ORS285 *ribBX* mutant strain. **A,** Comparison of the growth of *Aeschynomene evenia* plants inoculated with wild-type (wt) ORS285, ORS285 *ribBX,* ORS285 *ribBX* + pMG105 P_{ribBX}-*ribBX*, ORS285 *ribBX* + pMG105 P_{ribBX}-*ribB*, and ORS285 *ribBX* + pMG105 P_{ribBX}-*ribA*. Noninoculated plants (ni) were used as control. **B,** Mature nodules on *A. evenia* plants inoculated with ORS285, ORS285 *ribBX,* ORS285 *ribBX* + pMG105 P_{ribBX}-*ribBX*, ORS285 *ribBX* + pMG105 P_{ribBX}-*ribB*, and ORS285 *ribBX* + pMG105 P_{ribBX}-*ribA*. **C,** Number of root nodules on *A. evenia* plants inoculated with ORS285, ORS285 *ribBX,* ORS285 *ribBX* + pMG105 P_{ribBX}-*ribBX*, ORS285 *ribBX* + pMG105 P_{ribBX}-*ribB*, and ORS285 *ribBX* + pMG105 P_{ribBX}-*ribA*. The mean number of nodules per plant (n = 5) at 23 days postinfection (dpi) is presented. **D,** Acetylene-reducing activity of *A. evenia* plants inoculated with ORS285, ORS285 *ribBX,* ORS285 *ribBX* + pMG105 P_{ribBX}-*ribBX*, ORS285 *ribBX* + pMG105 P_{ribBX}-*ribB*, and ORS285 *ribBX* + pMG105 P_{ribBX}-*ribA* at 23 dpi. The mean amount of produced ethylene per hour and per plant (n = 5) is indicated. Error bars (C and D) represent standard errors of the mean and letters represent conditions with significant difference according to Tukey's test ($P < 0.05$).

As indicated above, *ribBX* encodes for a protein with a 3,4-DHBP synthase domain and a RibX domain with unknown function. To analyze whether both domains are required for the symbiotic interaction of the ORS285 strain with *A. evenia*, the *ribBX* mutant strain was transformed with plasmids expressing full-length RibBX (p*ribBX*), the 3,4-DHBP synthase domain (p*ribB*), and the RibX domain (p*ribX*). Plasmids expressing full-length RibBX and the RibB domain were able to complement the symbiotic phenotype of the *ribBX* mutant strain (Fig. 5A to D). This indicates that the RibB domain in RibBX is sufficient to obtain an efficient symbiotic interaction of ORS285 with *A. evenia* plants.

The *Aeschynomene* spp. that establish NF-independent symbiosis form a single clade that can be split into four subgroups (Chaintreuil et al. 2018). To investigate whether the requirement for a functional *ribBX* gene as found for *A. evenia* is a generality within this clade, we infected one species of each subgroup with the *ribBX* mutant strain. With all analyzed species, plants infected with the *ribBX* mutant strain had (i) nitrogen starvation symptoms, (ii) an increase in number of nodules as compared with plants infected with the WT, and (iii) low nitrogenase enzyme activity (Table 1). These data suggest that the functionality of the *ribBX* gene is obligatory for an efficient symbiotic interaction with NF-independent *Aeschynomene* spp.

In NF-dependent *Aeschynomene* spp., RibBX requirement depends on the host plant.

We also investigated the consequence of inactivating the *ribBX*, *gcdH*, *BRAD5118*, or *gntR-like* gene on *A. afraspera* plants, an *Aeschynomene* spp. that uses an NF-dependent process for symbiosis. Another characteristic of the symbiosis between ORS285 and *A. afraspera* is that, in this interaction, the ORS285 cells differentiate into elongated bacteroids (elongated bacteroids are characteristic for the interaction of ORS285 with all NF-dependent *Aeschynomene* host plants). For this, we infected *A. afraspera* with the different mutant strains and observed the effect on plant growth, nodule number, and nitrogenase enzyme activity at 20 dpi. In all analyzed phenotypic aspects, plants infected with the mutant strains were indistinguishable from plants infected with the WT strain (Fig. 6A to D). To analyze whether the *ribBX* gene is expressed in *A. afraspera*, we also inoculated this NF-dependent *Aeschynomene* sp. with the reporter strain, in which the *gusA* gene is placed under the control of the promoter region of the *ribBX* gene. As in nodules from *A. evenia* plants, nodules from *A. afraspera* plants infected with this reporter strain had high GUS activity, in contrast to nodules induced by the WT strain (Fig. 6E and F). Although 5-bromo-4-chloro-3-indoxyl-β-D-glucuronide cyclohexylammonium salt staining is a qualitative measurement for gene expression, we want to note that, by eye and under the same experimental conditions, no difference in color between the nodules of *A. evenia* and *A. afraspera* could be detected (Figs. 4C and 6F). This indicates that there is no correlation between the RibBX requirement for symbiosis and the expression in the nodules. The absence of an effect with the *ribBX* strain in *A. afraspera* plants was surprising because, with all tested NF-independent *Aeschynomene* spp., the symbiotic

interaction of this mutant was drastically affected (Fig. 3; Table 1). For this reason, we tested the *ribBX* mutant with another NF-dependent *Aeschynomene* sp., *A. nilotica*, which establishes an efficient symbiosis with the WT ORS285 strain. In contrast to *A. afraspera*, *A. nilotica* plants had nitrogen starvation symptoms, increased nodule numbers, and no nitrogenase enzyme activity when infected with the *ribBX* mutant (Fig. 7A to D). This indicates that, in the group of NF-dependent *Aeschynomene* spp., the requirement of RibBX activity to establish an efficient symbiosis varies with the host plant.

To investigate the contrasting phenotype of the *ribBX* mutant in symbiosis with *A. afraspera* and *A. nilotica* in more detail, we used the YFP-tagged version of the WT and *ribBX* mutant strain to study the bacteroid differentiation. In nodules of both NF-dependent *Aeschynomene* spp., ORS285 *ribBX* mutant cells differentiated like the WT cells into elongated bacteroids (Fig. 8B, D, F, and H). However, despite the differentiation of the *ribBX* mutant into elongated bacteroids in *A. nilotica* plants as observed at 7 dpi, most of the *ribBX* mutant-induced nodules observed at 21 dpi were hollow inside and displayed no GUS activity (Fig. 7F). This indicates that, despite the differentiation of the *ribBX* mutant into elongated bacteroids, the bacterial infection was not maintained and the nodules senesced very shortly after their formation.

DISCUSSION

The riboflavin biosynthesis pathway has been extensively studied, and all enzymes that compose this pathway are thought to be identified and well conserved in bacteria. Similar to other bacteria, the *Bradyrhizobium* ORS285 strain contains sequence homologs of the RibA and RibB enzymes that catalyze the initial step of two separate reactions that converge in the riboflavin synthesis pathway (Fig. 1A). However, as found in some bacteria, the RibB and RibA domains are fused and encoded by a single gene that was annotated as *ribBA*. Here, we show that the growth of an ORS285 strain in which the *ribBA* gene is inactivated is indistinguishable from the growth of the WT strain, indicating that the *ribBA* mutant still produced sufficient riboflavin to sustain growth (Fig. 1E and F). In addition, sequence analysis of the RibA domain and complementation experiments using an *E. coli ribA* mutant strain indicated that this domain does not have GTP cyclohydrolase II activity (Fig. 2A and B). The latter has also been observed for *ribBA* homologs from *Shewanella oneidensis*, *Pseudomonas putida*, *Vibrio parahaemolyticus*, and *Burkholderia cenocepacia* which, for that reason, have been renamed as *ribBX* (Brutinel et al. 2013). In accordance, we have renamed the ORS285 *ribBA* gene *ribBX* and the domain with homology to RibA the RibX domain. For *S. oneidensis* RibBX, it has been shown that the presence of the RibX domain decreases the 3,4-DHBP synthase activity of the RibB domain (Brutinel et al. 2013). In addition, recent experiments using purified *Acinetobacter baumannii* RibBX showed that FMN (one of the end products of riboflavin biosynthesis) drastically inhibits the 3,4-DHBP synthase activity (Wang et al. 2019). Structural modeling of FMN on the *A. baumannii* RibBX crystal structure indicated that the RibX domain can bind FMN. Based on this finding, it is hypothesized that FMN binding to the RibX domain allosterically regulates the enzyme activity of the RibB domain (Wang et al. 2019). These results indicate that the RibX domain has a regulatory function and explains why some of these domains originally annotated as "RibA" do not display the predicted GTP cyclohydrolase II enzyme activity.

The above results, and the absence of other genes encoding proteins with homology to RibA and RibB, suggest that ORS285 has other unknown enzymes with GTP cyclohydrolase II and 3,4-DHBP synthase activity or uses a different biosynthesis pathway to produce riboflavin. With respect to the RibB enzyme activity, studies have indicated that diacetyl (= butanedione/butane-2,3-dione) is able to replace 3,4-dihydroxybutanone in the riboflavin biosynthesis pathway (Crossley et al. 2007; Nakajima and Mitsuda 1984). Diacetyl is synthesized from pyruvate and the first step of the biosynthesis pathway is mediated by thiamine pyrophosphate (TPP). Interestingly, in *Bradyrhizobium* ORS285 and several other bacteria, the gene *thiL*, encoding the enzyme catalyzing the last step in TPP biosynthesis, is found close to *rib* genes (Fig. 1B). Thus, using diacetyl instead of 3,4-dihydroxybutanone to synthesize riboflavin could, in part, explain why the absence of 3,4-DHBP synthase activity in the ORS285 *ribBX* strain does not lead to riboflavin auxotrophy. Interestingly, an *Ensifer meliloti ribBA* mutant has also been shown not to be a riboflavin auxotroph and no additional *ribBA*, *ribA*, or *ribB* genes could be identified (Yurgel et al. 2014). Thus, the presence of an unconventional route or alternative enzymes to synthesize riboflavin could be more common in rhizobia and requires further research in the future.

In several bacteria, *ribBA*/*ribBX* mutants have been shown to secrete less or no riboflavin into the extracellular medium (Brutinel et al. 2013; Worst et al. 1998; Yang et al. 2002; Yurgel et al. 2014). In contrast to *E. meliloti,* laboratory-grown ORS285 WT cells secrete very low levels of riboflavin into the culture medium (riboflavin fluorescence just above the fluorescent levels of the noninoculated growth medium), and these

Table 1. Characteristics of the symbiotic interaction between the wild type (WT) and the *ribBX* mutant of *Bradyrhizobium* ORS285 and different Nod-factor (NF)-independent and NF-dependent *Aeschynomene* spp.[a]

	Growth stimulation plants		Mean number of nodules/plant		Leghemoglobin		Nitrogenase enzyme activity (nmol ethylene/plant/h)	
Plant species	**WT**	***ribBX***	**WT**	***ribBX***	**WT**	***ribBX***	**WT**	***ribBX***
NF-independent								
Aeschynomene evenia	+++	–	29 ± 4	56 ± 8	Yes	No	450 ± 34	4 ± 1
A. sensitiva	+++	–	29 ± 5	43 ± 4	Yes	No	319 ± 91	83 ± 30
A. deamii	+++	–	48 ± 8	53 ± 4	Yes	No	618 ± 293	162 ± 70
A. tambacoudensis	+++	–	8 ± 3	20 ± 11	Yes	No	70 ± 30	nd
NF-dependent								
A. afraspera	+++	+++	25 ± 2	25 ± 1	Yes	Yes	702 ± 33	790 ± 96
A. nilotica	+++	–	12 ± 3	42 ± 2	Yes	No	577 ± 106	33 ± 12

[a] Seedlings of different *Aeschynomene* spp. were inoculated with wild-type (WT) ORS285 and ORS285 *ribBX*. At 23 days postinfection (dpi), the plant growth was compared with noninoculated control plants and the mean nodule number, mature nodule phenotype, and mean nitrogenase enzyme activity, as analyzed by the acetylene reduction assay, was determined. Symbols: +++ indicates no nitrogen-starvation signs and plants are much better developed than the noninoculated control plants, – indicates no difference with noninoculated control plants, nd = not detectable, and ± indicates the standard error of the mean.

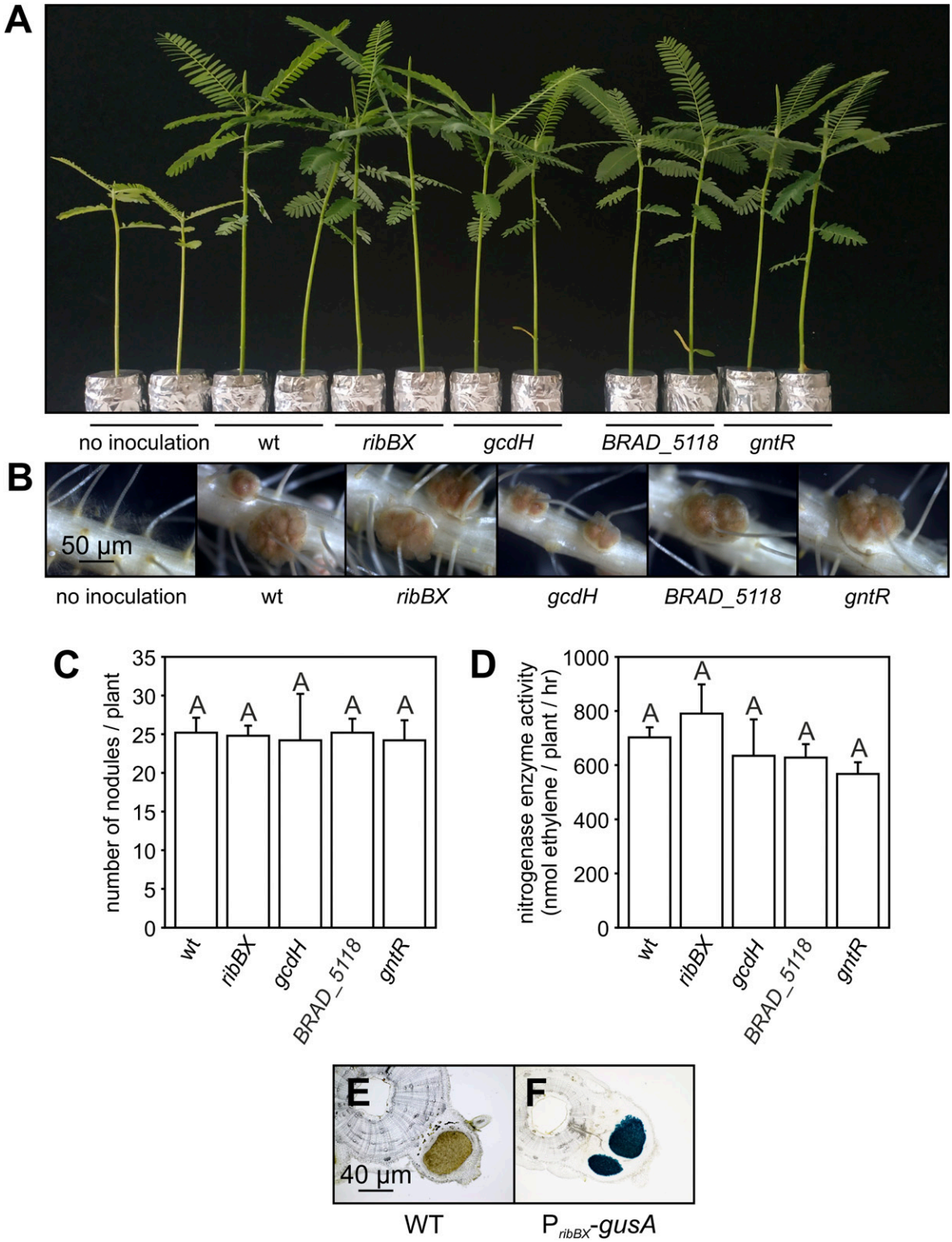

Fig. 6. ORS285 *ribBX* does not affect the symbiotic interaction with *Aeschynomene afraspera* (LSTM number 1). **A,** Comparison of the growth of *A. afraspera* plants inoculated with wild-type (wt) ORS285, ORS285 *ribBX*, ORS285 *gcdH*, ORS285 *BRAD5118*, and ORS285 *gntR*. Noninoculated plants (ni) were used as control. **B,** Mature nodules on *A. afraspera* plants inoculated with ORS285, ORS285 *ribBX*, ORS285 *gcdH*, ORS285 *BRAD5118*, and ORS285 *gntR*. **C,** Number of root nodules on *A. afraspera* plants inoculated with ORS285, ORS285 *ribBX*, ORS285 *gcdH*, ORS285 *BRAD5118*, and ORS285 *gntR*. The mean number of nodules per plant ($n = 5$) at 23 days postinfection (dpi) is presented. **D,** Acetylene-reducing activity of *A. afraspera* plants inoculated with ORS285, ORS285 *ribBX*, ORS285 *gcdH*, ORS285 *BRAD5118*, and ORS285 *gntR* at 23 dpi. The mean amount of produced ethylene per hour and per plant ($n = 5$) is indicated. Error bars (C and D) represent standard errors of the mean and letters represent conditions with significant difference according to Tukey's test ($P < 0.05$). *RibBX* promoter activity in nodules of *A. evenia*. *A. evenia* plants were infected with **E,** the wild-type (WT) or **F,** P_{ribBX}-*gusA* reporter strain and, at 15 dpi, the β-glucuronidase activity in 70 µM nodule sections was determined by 5-bromo-4-chloro-3-indoxyl-β-D-glucuronide cyclohexylammonium salt staining.

levels were hardly affected with the *ribBA* mutant strain (Supplementary Fig. S2). Due to these very low levels of riboflavin secretion, we were unable to draw a conclusion concerning an eventual role of the ORS285 RibBX protein in riboflavin secretion. In contrast to other rhizobia for which abundant riboflavin secretion have been shown, photosynthetic bradyrhizobia are very slow-growing bacteria. Also, riboflavin has been shown to trigger (prime) the immune system of plants (Nie and Xu 2016). The very slow growth under laboratory conditions and not using NFs (which have been shown to suppress the plant innate immune response) (Liang et al. 2013) in certain symbiotic interactions could be reasons why ORS285 cells do secrete very low amounts of riboflavin into the extracellular medium. In all bradyrhizobia, *ribBX* forms an operon with the *gcdH* gene which encodes for a glutaryl-CoA dehydrogenase (GDH) that converts glutaryl-CoA into crotonyl-CoA and carbon dioxide (CO_2), a reaction that plays a role in the degradation of fatty acids, lysine, and benzoate but also in the metabolism of tryptophan (Blázquez et al. 2008; Hildebrandt et al. 2015; Revelles et al. 2005). GDH belongs to the acetyl-CoA dehydrogenase gene family, whose members contain a derivative of riboflavin, FAD, as cofactor. Upon oxidation of the substrate, the FAD cofactor accepts the electron and subsequently transfers it to an electron-transfer flavoprotein to finish the reaction cycle. Thus, although we could not demonstrate a key role for ORS285 RibBX in riboflavin biosynthesis under laboratory conditions, the *ribBX* gene context suggests that it could play an essential role when the main biosynthesis pathway does not produce sufficient riboflavin to support metabolic pathways in which GcdH plays a role.

In this study, we showed that RibBX is required for an efficient symbiotic interaction of *Bradyrhizobium* ORS285 with certain and, in particular, NF-independent *Aeschynomene* spp. (Fig. 3; Table 1). With these species, plants infected with the ORS285 *ribBX* mutant formed nodules but these nodules were unable to fix nitrogen (Fix$^-$ phenotype). The absence of

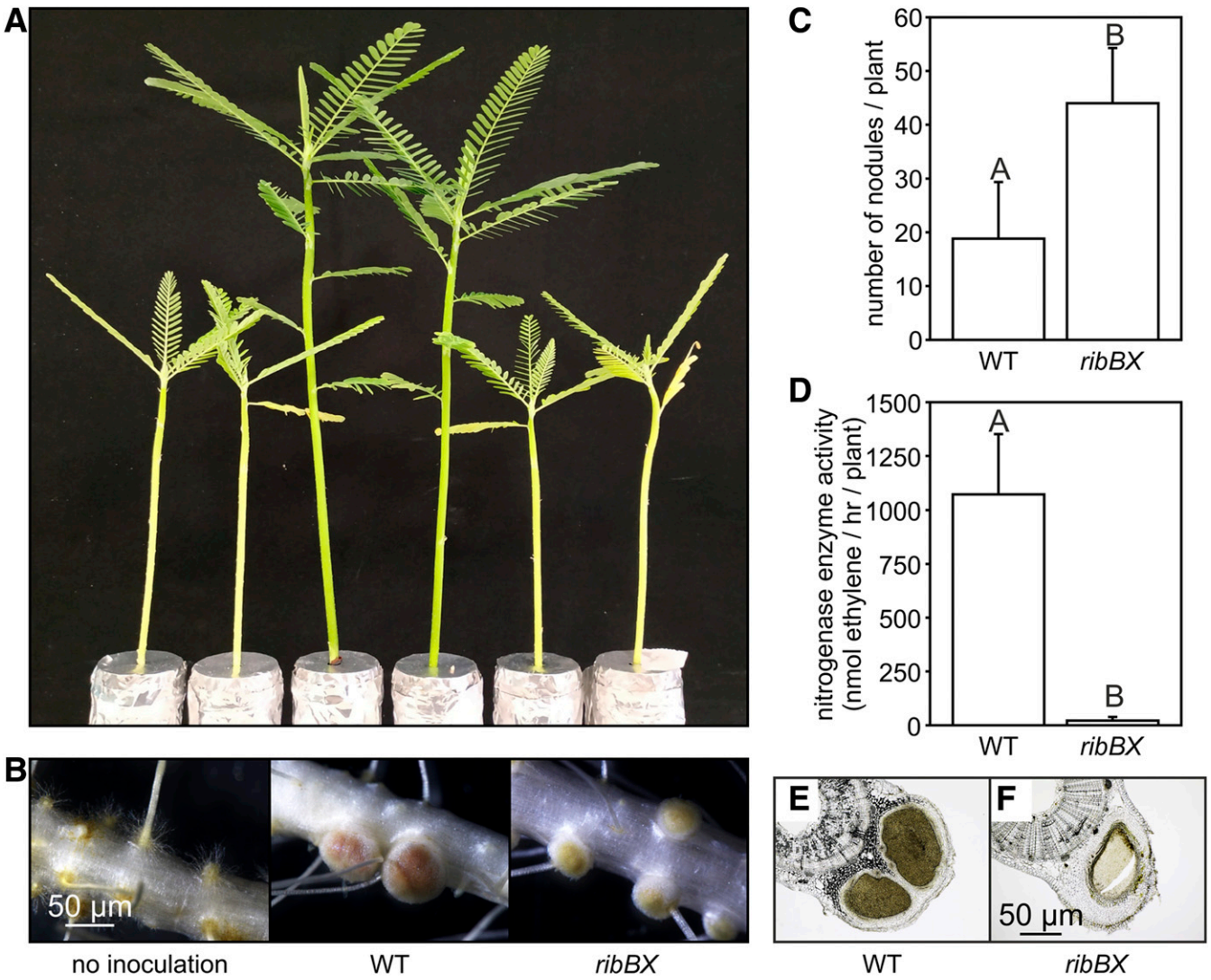

Fig. 7. ORS285 *ribBX* deletion affects the symbiotic interaction with *Aeschynomene nilotica* (IRRI 014040). **A,** Comparison of the growth of *A. nilotica* plants inoculated with wild-type (WT) ORS285 and ORS285 *ribBX* at 23 days postinfection (dpi). Noninoculated plants (ni) were used as control. **B,** Mature nodules on *A. nilotica* plants inoculated with ORS285 and ORS285 *ribBX*. White-colored nodules on *A. nilotica* plants inoculated with the ORS285 *ribBX* strain are indicated with a black arrow. **C,** Number of root nodules on *A. nilotica* plants inoculated with ORS285 and ORS285 *ribBX*. The mean number of nodules per plant ($n = 5$) at 23 dpi is presented. **D,** Acetylene-reducing activity of *A. nilotica* plants inoculated with *Bradyrhizobium* ORS285 and ORS285 *ribBX* at 23 dpi. The mean amount of produced ethylene per hour and per plant ($n = 5$) is indicated. Error bars (C and D) represent standard errors of the mean and letters represent conditions with significant difference according to Tukey's test ($P < 0.05$). β-Glucuronidase activity in *A. nilotica* nodules induced by **E,** wild-type (WT) and **F,** the *ribBX* mutant strain of *Bradyrhizobium* ORS285. Nodule sections (70 µM) were stained for 6 h with 5-bromo-4-chloro-3-indoxyl-β-D-glucuronide cyclohexylammonium salt.

nitrogenase enzyme activity seems not be related to a dysfunction of the nitrogenase enzyme complex itself because the ORS285 *ribBX* mutant is able to fix nitrogen when grown under free-living conditions (Fig. 4A). The Fix$^-$ phenotype of the *ribBX* mutant could be complemented by expressing the complete RibBX protein or the RibB domain but not by the RibX domain (Fig. 5). This suggests that the observed symbiotic defect was due to the absence of the RibB domain alone. Microscopic analysis of NF-independent *Aeschynomene evenia* nodules showed that the *ribBX* mutant infects plant cells intracellularly but that the bacteria did not differentiate into spherical bacteroids, which are characteristic for NF-independent *Aeschynomene* spp. (Fig. 4L). In addition, the nodules senesced early and, at 21 dpi, the majority of nodules on *ribBX*-infected plants were completely devoid of bacteria (Fig. 4E). Thus, ORS285 RibBX or, rather, the RibB domain seems to be required for the persistence of the intracellular infection in *Aeschynomene* plants. Interestingly, a link between riboflavin biosynthesis and intracellular survival in eukaryotic cells has previously been shown for *Brucella abortus* (Bonomi et al. 2010). As indicated above, the gene context of *ribBX* suggests that riboflavin biosynthesis via RibBX is employed when the bacterium uses metabolic pathways that require GcdH enzyme activity. However, inactivation of the *gcdH* gene had no effect on the symbiotic interaction of ORS285 with *Aeschynomene* legumes (Figs. 3 and 6). In this context, it should be noted that *Bradyrhizobium* ORS285, in addition to *gcdH*, contains many other genes that encode for proteins which belong to the same gene family as GcdH and of which the function is unknown. Thus, it is highly possible that the absence of a symbiotic phenotype for the *gcdH* mutant is due to functional redundancy and that one of these putative acetyl-CoA dehydrogenases converts the formed glutaryl-CoA during symbiosis. Alternatively, *Bradyrhizobium* ORS285 could contain an additional glutarate catabolic pathway, as recently discovered in *P. putida* KT2440. In this pathway, glutarate is not acetylated into glutaryl-CoA but in a reaction with 2-ketoglutarate converted into L-2-hydroxyglutarate and succinate (Zhang et al. 2018). Taken together, as was done by the authors in the *B. abortus* study, at this stage we are unable to pinpoint a specific biological process during the intracellular infection for which riboflavin biosynthesis is required.

Intriguingly, when the NF-dependent *Aeschynomene* sp. *A. afraspera* was infected with the ORS285 *ribBX* mutant, no symbiotic defect was observed (Fig. 6). This means that ORS285 does not need RibBX activity for interacting with *A. afraspera*, or that this plant species supplies the bacterium with the required riboflavin. A similar difference in symbiotic interaction has previously described for an ORS285 *nifV* mutant (Nouwen et al. 2017). In this case, we were able to demonstrate that *A. afraspera* expresses a nodule-specific homocitrate synthase that provides the bacteria with homocitrate so that it can form an active nitrogenase enzyme complex. Plants synthesize riboflavin using enzymes that are similar to the ones found in bacteria (Fischer and Bacher 2006). Analysis of genomic and transcriptomic data of *A. evenia* and *A. afraspera* showed that they have multiple copies of genes encoding RibBA-like proteins (Supplementary Table S4). In both *A. evenia* and *A. afraspera*, some of these genes showed a somewhat increased expression in nodule tissue. However, none of the RibBA orthologs showed a nodule-specific expression profile such as we have found for FEN1 (Nouwen et al. 2017). Thus, the nodule-specific expression of an RibBA ortholog in *A. afraspera* to provide riboflavin to the symbiotic bacterium is likely not the reason why no effect is observed in the interaction of this plant species with the ORS285 *ribBX* mutant.

The nonrequirement of bacterial RibBX in symbiosis is not a universal characteristic in NF-dependent *Aeschynomene* spp. because, in the second species tested, *A. nilotica*, the *ribBX* mutation had a drastic negative impact on the symbiotic interaction (Fig. 7). Such variation has also been observed, for instance, for the interaction of an *R. trifolii* riboflavin auxotroph with different clover species (genus *Trifolium*) (Pankhurst et al. 1974; Schwinghamer 1970). This indicates that bacterial riboflavin requirements in certain NF-dependent interactions are dependent on the host plant genotype. As an essential component of flavoproteins, riboflavin derivatives play important roles in many different physiological processes. Consequently, environmental factors such as oxidative or nitrosative stress, iron or oxygen availability, available growth substrates, and eventual toxic compounds to be inactivated are expected to have a great impact on how much riboflavin has to be synthesized by the bacterium. A specific environmental condition in the nodule tissue of certain *Aeschynomene* spp. could mean that the bacterium requires the RibBX protein to increase the total amount of riboflavin synthesized or, alternatively, to compensate for a reduced synthesis via a thus-far-unidentified pathway. Given the complexity of the rhizobium–legume interaction, we expect that the total amount of riboflavin required during symbiosis (and the pathway used to synthesize it) is determined by multiple factors. This could explain the host-dependent phenotype as observed in NF-dependent symbiosis but also means that the existence of NF-independent interactions in which bacterial RibBX is not required cannot be completely excluded.

Taken together, this study shows that the RibBX protein plays an important role in the symbiotic interaction of *Bradyrhizobium* ORS285 with the majority of the tested *Aeschynomene* spp. In addition, as found for *E. meliloti* (Yurgel et al. 2014), inactivation of *ribB(A)X* did not result in riboflavin auxotrophy, whereas no other copies of genes homologous to *ribA* and *ribB* are present. Future studies are required to obtain a better understanding of riboflavin biosynthesis in rhizobia and bradyrhizobia in general and the requirement of riboflavin during symbiosis.

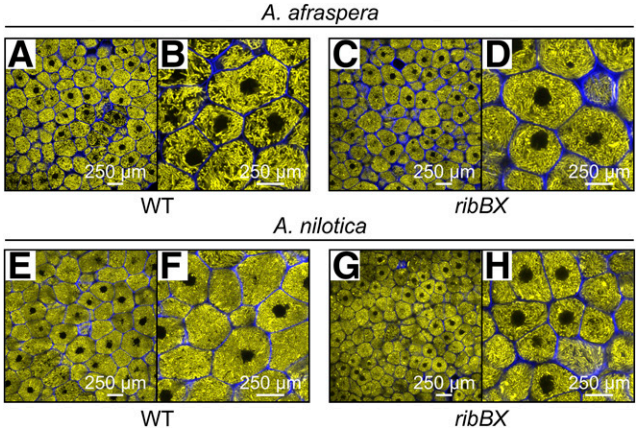

Fig. 8. Confocal microscopic analysis of nodules induced by wild-type (WT) ORS285 and ORS285 *ribBX* mutant on **A** to **D,** *Aeschynomene afraspera* and **E** to **H,** *A. nilotica* plants. The ORS285 and ORS285 *ribBX* bacteriods are elongated in both *Aeschynomene* spp.

MATERIALS AND METHODS

Bacterial strains and growth conditions.

Tables of strains and plasmids used in this study can be found in the supplementary materials (Supplementary Tables S1 and S2). *Bradyrhizobium* ORS285 (Molouba et al. 1999) and derivatives were grown at 28°C in modified yeast extract mannitol medium (YM) (Giraud et al. 2000) or a minimal BNM-B medium to which no riboflavin was added (Podlešáková et al. 2013).

Escherichia coli riboflavin auxotrophs (Bandrin et al. 1983) were obtained from the Coli Genetic Stock Center. *E. coli* strains were grown in Luria-Bertani medium or a minimal M9 medium at 37°C. When required, the media were supplemented with ampicillin (50 to 100 μg/ml), kanamycin (50 to 100 μg/ml), cefotaxime (20 μg/ml), spectinomycine (20 to 200 μg/ml), or 500 μM riboflavin.

Construction of mutant and reporter strains of *Bradyrhizobium* ORS285.

All DNA fragments were amplified using primers as listed in Supplementary Table S3. To construct *ribBX*, *gcdH*, *BRAD5118*, and *gntR* insertional mutants, 312 to 382 bp of the internal sequence of each gene was amplified by PCR. The resulting fragments were isolated, cloned into plasmid pGEM-T Easy (Promega Corp.), and transformed into thermocompetent *E. coli* XL2-Blue cells (Agilent). Correct clones were verified by sequence analysis. The internal gene fragments in pGEM-T Easy were excised with *Sal*I-*Bam*HI and ligated into suicide vector pJG194-PnodA-*gusA* (*ribBX*, *gcdH*, and *BRAD5118*) (Supplementary Materials) or pJG194 (*gntR*) (Griffitts and Long 2008) digested with *Sal*I-*Bam*HI. After transformation into *E. coli* XL2-Blue cells, correct clones were selected via kanamycin resistance (50 μg/ml) and subsequent DNA restriction enzyme analysis. To construct a *ribBX* reporter strain, the 276-bp region upstream of *ribBX* was amplified by PCR, cloned into pGEM-T Easy, and transformed into *E. coli* XL2-Blue cells. After verification by sequence analysis, the promoter fragment was excised with *Sal*I-*Bam*HI and ligated into suicide vector pJG194-PnodA-*gusA* digested with the same enzymes. After transformation into *E. coli* XL2-Blue cells, correct clones were selected as described above. Plasmids were transformed into $CaCl_2$-competent *E. coli* S17-1 cells (Simon et al. 1983) and mobilized into *Bradyrhizobium* ORS285 using the biparental mating protocol, as previously described (Podlešáková et al. 2013). Correct insertion of the plasmids was verified by PCR. To construct sYFP-tagged derivatives, plasmid pMG105-Paph-sYFP-specR (for construction, see Supplementary Materials) was transformed into electrocompetent *Bradyrhizobium* ORS285 (mutant) cells and, after transformation, plasmid-containing clones were selected via spectinomycine resistance (200 μg/ml) and sYFP fluorescence.

Complementation of the ORS285 *ribBX* mutant.

Complementation of the ORS285 *ribBX* mutant was tested with different DNA constructs: (i) construct A, consisting of the *ribBX* promoter region plus complete *ribBX* gene; (ii) construct B, consisting of the *ribBX* promoter region plus the RibB domain; and (iii) the *ribBX* promoter region plus the RibX domain. These DNA regions were PCR amplified using primers that can be found in Supplementary Table S3 and cloned into the pMG105-*specR* plasmid (Supplementary Materials) that contains the spectinomycine resistance gene. The pMG105 plasmid replicates and is stable in the ORS285 strain. To construct the plasmid in which the RibB domain has been deleted, the promoter region plus the first 12 nucleotides of *ribBX* and the RibX domain were PCR amplified and subsequently fused using overlapping PCR. The constructed plasmids (pMG105-P_{ribBX}-*ribBX*, pMG105-P_{ribBX}-*ribB*, and pMG105-P_{ribBX}-*ribX*) were introduced into electrocompetent cells of the ORS285 *ribBX* mutant by electroporation. Strains containing plasmids were selected on YM plates supplemented with spectinomycine at 200 μg/ml and kanamycine at 50 μg/ml.

Complementation of *E. coli ribA* and *ribB* mutants.

For complementation of *E. coli* riboflavin auxotroph mutants, *ribBX*, the *ribB* domain, and the *ribX* domain were PCR amplified from plasmids pMG105-P_{ribBX}-*ribBX*, pMG105-P_{ribBX}-*ribB*, and pMG105-P_{ribBX}-*ribX*, respectively, using primers as indicated in Supplementary Table S3. The resulting fragments were cloned into pGEM-T Easy and transformed into *E. coli* XL2-Blue cells, and correct clones were verified using DNA restriction enzyme analysis and DNA sequencing. Subsequently, the genes were excised from pGEM-T Easy by *Bam*HI-*Hin*dIII digestion and cloned into plasmid pJF118 E/H (Fürste et al. 1986) digested with the same enzymes. After transformation into *E. coli* XL2-Blue cells, correct clones were selected using DNA restriction enzyme analysis. For complementation studies, the different plasmids and pJF118 E/H were transformed into $CaCl_2$-competent cells of BSV11 (*ribB11::Tn5*) and BSV18 (*ribA18::Tn5*), respectively.

Plant growth and acetylene reduction assay.

Aeschynomene spp. used in this study were *A. evenia* (CIAT22838; Malawi), *A. deamii* (LSTM number 24; Mexico), *A. tambacoudensis* (LSTM number 60; Senegal), *A sensitiva* (LSTM number 28; Senegal), *A. afraspera* (LSTM number 1; Senegal), and *A. nilotica* (IRRI 014040; Senegal). Sterilization of seed, germination, plant growth, and inoculation with bacterial strains were as described (Nouwen et al. 2017). At the indicated times after inoculation (as specified in the figure legends), photos of plants were taken, the number of nodules on the roots were counted, and the ARA was used to measure the nitrogenase enzyme activity (Podlešáková et al. 2013). Time points of analysis were chosen such that there was a clear difference in growth phenotype between noninoculated and (WT) inoculated plants.

Microscopy.

For confocal microscopy, root sections containing nodules were harvested and rinsed with distilled water. The rinsed root sections were fixed overnight with 4% (wt/vol) paraformaldehyde in phosphate-buffered saline (PBS) at room temperature. The fixed root sections were washed three times with PBS, embedded in 5% agar, and sectioned (50 to 70 μM) using a vibratome (VT1000S; Leica, Nanterre, France). Nodules induced by sYFP-tagged strains were analyzed as described by Bonaldi et al. (2011). To determine the GUS activity in nodules formed by the mutant and P_{ribBX}-reporter strains, fresh nodules were embedded in 5% agarose and sectioned (50 to 70 μM) using a vibratome (VT1000S; Leica). Nodule sections were incubated for 30 min in GUS assay buffer (Bonaldi et al. 2011) at 37°C. After staining, the sections were washed three times with water, mounted on microscope slides, and observed under bright-field illumination with a macroscope (Nikon AZ100; Champigny-sur-Marne, France).

In vitro nitrogenase enzyme activity.

To determine the nitrogenase enzyme activity under free-living conditions, *Bradyrhizobium* ORS285 and ORS285 *ribBX* were grown in 9-ml vacuette tubes (reference 455001; Greiner Bio-One) containing 2 ml of BNM-B medium without riboflavin supplementation. To avoid overpressure, 0.9 ml of air was removed before injecting the same volume of 100% acetylene. The cultures were incubated at 28°C and, at 7 dpi, 1-ml gas samples were analyzed for ethylene production by gas chromatography and the optical density (at 600 nm) of the culture was determined (Nouwen et al. 2017).

AUTHOR-RECOMMENDED INTERNET RESOURCE

Coli Genetic Stock Center: https://cgsc.biology.yale.edu

LITERATURE CITED

Abbas, C. A., and Sibirny, A. A. 2011. Genetic control of biosynthesis and transport of riboflavin and flavin nucleotides and construction of robust biotechnological producers. Microbiol. Mol. Biol. Rev. 75:321-360.

Balasubramanian, R., Levinson, B. T., and Rosenzweig, A. C. 2010. Secretion of flavins by three species of methanotrophic bacteria. Appl. Environ. Microbiol. 76:7356-7358.

Bandrin, S. V., Rabinovich, P. M., and Stepanov, A. I. 1983. Tri gruppy stsepleniia genov biosinteza riboflavina *Escherichia coli* [Three linkage groups of the genes of riboflavin biosynthesis in *Escherichia coli]*. Genetika 19:1419-1425.

Blázquez, B., Carmona, M., García, J. L., and Díaz, E. 2008. Identification and analysis of a glutaryl-CoA dehydrogenase-encoding gene and its cognate transcriptional regulator from *Azoarcus* sp. CIB. Environ. Microbiol. 10:474-482.

Bonaldi, K., Gargani, D., Prin, Y., Fardoux, J., Gully, D., Nouwen, N., Goormachtig, S., and Giraud, E. 2011. Nodulation of *Aeschynomene afraspera* and *A. indica* by photosynthetic *Bradyrhizobium* Sp. strain ORS285: The *nod*-dependent versus the *nod*-independent symbiotic interaction. Mol. Plant-Microbe Interact. 24:1359-1371.

Bonaldi, K., Gourion, B., Fardoux, J., Hannibal, L., Cartieaux, F., Boursot, M., Vallenet, D., Chaintreuil, C., Prin, Y., Nouwen, N., and Giraud, E. 2010. Large-scale transposon mutagenesis of photosynthetic *Bradyrhizobium* sp. strain ORS278 reveals new genetic loci putatively important for nod-independent symbiosis with *Aeschynomene indica*. Mol. Plant-Microbe Interact. 23:760-770.

Bonomi, H. R., Marchesini, M. I., Klinke, S., Ugalde, J. E., Zylberman, V., Ugalde, R. A., Comerci, D. J., and Goldbaum, F. A. 2010. An atypical riboflavin pathway is essential for *Brucella abortus* virulence. PLoS One 5:e9435. doi:

Brutinel, E. D., Dean, A. M., and Gralnick, J. A. 2013. Description of a riboflavin biosynthetic gene variant prevalent in the phylum Proteobacteria. J. Bacteriol. 195:5479-5486.

Chaintreuil, C., Perrier, X., Martin, G., Fardoux, J., Lewis, G. P., Brottier, L., Rivallan, R., Gomez-Pacheco, M., Bourges, M., Lamy, L., Thibaud, B., Ramanankierana, H., Randriambanona, H., Vandrot, H., Mournet, P., Giraud, E., and Arrighi, J.-F. 2018. Naturally occurring variations in the *nod*-independent model legume *Aeschynomene evenia* and relatives: A resource for nodulation genetics. BMC Plant Biol. 18:54.

Christie, J. M., Blackwood, L., Petersen, J., and Sullivan, S. 2015. Plant flavoprotein photoreceptors. Plant Cell Physiol. 56:401-413.

Crossley, R. A., Gaskin, D. J. H., Holmes, K., Mulholland, F., Wells, J. M., Kelly, D. J., van Vliet, A. H. M., and Walton, N. J. 2007. Riboflavin biosynthesis is associated with assimilatory ferric reduction and iron acquisition by *Campylobacter jejuni*. Appl. Environ. Microbiol. 73: 7819-7825.

Czernic, P., Gully, D., Cartieaux, F., Moulin, L., Guefrachi, I., Patrel, D., Pierre, O., Fardoux, J., Chaintreuil, C., Nguyen, P., Gressent, F., Da Silva, C., Poulain, J., Wincker, P., Rofidal, V., Hem, S., Barrière, Q., Arrighi, J.-F., Mergaert, P., and Giraud, E. 2015. Convergent evolution of endosymbiont differentiation in dalbergioid and inverted repeat-lacking clade legumes mediated by nodule-specific cysteine-rich peptides. Plant Physiol. 169:1254-1265.

da Silva Neto, J. F., Lourenço, R. F., and Marques, M. V. 2013. Global transcriptional response of *Caulobacter crescentus* to iron availability. BMC Genomics 14:549.

Dunlap, P. 2014. Biochemistry and genetics of bacterial bioluminescence. Adv. Biochem. Eng. Biotechnol. 144:37-64.

Fischer, M., and Bacher, A. 2006. Biosynthesis of vitamin B2 in plants. Physiol. Plant. 126:304-318.

Fürste, J. P., Pansegrau, W., Frank, R., Blöcker, H., Scholz, P., Bagdasarian, M., and Lanka, E. 1986. Molecular cloning of the plasmid RP4 primase region in a multi-host-range tacP expression vector. Gene 48:119-131.

García-Angulo, V. A. 2017. Overlapping riboflavin supply pathways in bacteria. Crit. Rev. Microbiol. 43:196-209.

Giraud, E., Hannibal, L., Fardoux, J., Verméglio, A., and Dreyfus, B. 2000. Effect of *Bradyrhizobium* photosynthesis on stem nodulation of *Aeschynomene sensitiva*. Proc. Natl. Acad. Sci. U.S.A. 97:14795-14800.

Giraud, E., Moulin, L., Vallenet, D., Barbe, V., Cytryn, E., Avarre, J.-C., Jaubert, M., Simon, D., Cartieaux, F., Prin, Y., Bena, G., Hannibal, L., Fardoux, J., Kojadinovic, M., Vuillet, L., Lajus, A., Cruveiller, S., Rouy, Z., Mangenot, S., Segurens, B., Dossat, C., Franck, W. L., Chang, W.-S., Saunders, E., Bruce, D., Richardson, P., Normand, P., Dreyfus, B., Pignol, D., Stacey, G., Emerich, D., Verméglio, A., Médigue, C., and Sadowsky, M. 2007. Legumes symbioses: Absence of *Nod* genes in photosynthetic bradyrhizobia. Science 316:1307-1312.

Griffitts, J. S., and Long, S. R. 2008. A symbiotic mutant of *Sinorhizobium meliloti* reveals a novel genetic pathway involving succinoglycan biosynthetic functions. Mol. Microbiol. 67:1292-1306.

Haase, I., Gräwert, T., Illarionov, B., Bacher, A., and Fischer, M. 2014. Recent advances in riboflavin biosynthesis. Pages 15-40 in: Flavins and Flavoproteins. S. Weber and E. Schleicher, eds. Methods in Molecular Biology, vol. 1146. Humana Press, New York, NY, U.S.A.

Hildebrandt, T. M., Nunes Nesi, A., Araújo, W. L., and Braun, H. P. 2015. Amino acid catabolism in plants. Mol. Plant 8:1563-1579.

Kelly, M. J. S., Ball, L. J., Krieger, C., Yu, Y., Fischer, M., Schiffmann, S., Schmieder, P., Kühne, R., Bermel, W., Bacher, A., Richter, G., and Oschkinat, H. 2001. The NMR structure of the 47-kDa dimeric enzyme 3,4-dihydroxy-2-butanone-4-phosphate synthase and ligand binding studies reveal the location of the active site. Proc. Natl. Acad. Sci. U.S.A. 98:13025-13030.

Liang, Y., Cao, Y., Tanaka, K., Thibivilliers, S., Wan, J., Choi, J., Kang, Ch., Qiu, J., and Stacey, G. 2013. Nonlegumes respond to rhizobial Nod factors by suppressing the innate immune response. Science 341:1384-1387.

Liao, D.-I., Calabrese, J. C., Wawrzak, Z., Viitanen, P. V., and Jordan, D. B. 2001. Crystal structure of 3,4-dihydroxy-2-butanone 4-phosphate synthase of riboflavin biosynthesis. Structure 9:11-18.

Molouba, F., Lorquin, J., Willems, A., Hoste, B., Giraud, E., Dreyfus, B., Gillis, M., de Lajudie, P., and Masson-Boivin, C. 1999. Photosynthetic bradyrhizobia from *Aeschynomene* spp. are specific to stem-nodulated species and form a separate 16S ribosomal DNA restriction fragment length polymorphism group. Appl. Environ. Microbiol. 65:3084-3094.

Nakajima, K., and Mitsuda, H. 1984. Possibility of diacetyl and related compounds as the 4-carbon compound necessary for the formation of riboflavin in *Ashbya gossypii*. Acta Vitaminol. Enzymol. 6:271-282.

Nie, S., and Xu, H. 2016. Riboflavin-induced disease resistance requires the mitogen-activated protein kinases 3 and 6 in *Arabidopsis thaliana*. PLoS One 11:e0153175. doi:

Nouwen, N., Arrighi, J.-F., Cartieaux, F., Chaintreuil, C., Gully, D., Klopp, C., and Giraud, E. 2017. The role of rhizobial (NifV) and plant (FEN1) homocitrate synthases in *Aeschynomene*/photosynthetic *Bradyrhizobium* symbiosis. Sci. Rep. 7:448.

Pankhurst, C. E., Schwinghamer, E. A., Thorne, S. W., and Bergersen, F. J. 1974. The flavin content of clovers relative to symbiosis with a riboflavin-requiring mutant of *Rhizobium trifoli*. Plant Physiol. 53:198-205.

Podlešáková, K., Fardoux, J., Patrel, D., Bonaldi, K., Novák, O., Strnad, M., Giraud, E., Spíchal, L., and Nouwen, N. 2013. Rhizobial synthesized cytokinins contribute to but are not essential for the symbiotic interaction between photosynthetic Bradyrhizobia and *Aeschynomene* legumes. Mol. Plant-Microbe Interact. 26:1232-1238.

Ren, J., Kotaka, M., Lockyer, M., Lamb, H. K., Hawkins, A. R., and Stammers, D. K. 2005. GTP cyclohydrolase II structure and mechanism. J. Biol. Chem. 280:36912-36919.

Revelles, O., Espinosa-Urgel, M., Fuhrer, T., Sauer, U., and Ramos, J. L. 2005. Multiple and interconnected pathways for L-lysine catabolism in *Pseudomonas putida* KT2440. J. Bacteriol. 187:7500-7510.

Rigali, S., Derouaux, A., Giannotta, F., and Dusart, J. 2002. Subdivision of the helix-turn-helix GntR family of bacterial regulators in the FadR, HutC, MocR, and YtrA subfamilies. J. Biol. Chem. 277:12507-12515.

Schwinghamer, E. 1970. Requirement for riboflavin for effective symbiosis on clover by an auxotrophic mutant strain of *Rhizobium trifolii*. Aust. J. Biol. Sci. 23:1187.

Simon, R., Priefer, U., and Pühler, A. 1983. A broad host range mobilization system for *in vivo* genetic engineering: Transposon mutagenesis in Gram negative bacteria. Bio/Technology 1:784-791.

Tagua, V. G., Pausch, M., Eckel, M., Gutiérrez, G., Miralles-Durán, A., Sanz, C., Eslava, A. P., Pokorny, R., Corrochano, L. M., and Batschauer, A. 2015. Fungal cryptochrome with DNA repair activity reveals an early stage in cryptochrome evolution. Proc. Natl. Acad. Sci. U.S.A. 112: 15130-15135.

Tan, Y., Liu, Z.-Y., Liu, Z., Zheng, H.-J., and Li, F.-L. 2015. Comparative transcriptome analysis between *csrA*-disruption *Clostridium acetobutylicum* and its parent strain. Mol. Biosyst. 11:1434-1442.

Taniguchi, H., and Wendisch, V. F. 2015. Exploring the role of sigma factor gene expression on production by *Corynebacterium glutamicum*: Sigma factor H and FMN as example. Front. Microbiol. 6:740.

Wang, C., Reid, J. B., and Foo, E. 2018. The art of self-control—Autoregulation of plant–microbe symbioses. Front. Plant Sci. 9:988.

Wang, J., Lonergan, Z. R., Gonzalez-Gutierrez, G., Nairn, B. L., Maxwell, C. N., Zhang, Y., Andreini, C., Karty, J. A., Chazin, W. J., Trinidad, J. C., Skaar, E. P., and Giedroc, D. P. 2019. Multi-metal restriction by Calprotectin impacts *de novo* flavin biosynthesis in *Acinetobacter baumannii*. Cell Chem. Biol. 26:745-755.e7.

Winkler, W. C., Cohen-Chalamish, S., and Breaker, R. R. 2002. An mRNA structure that controls gene expression by binding FMN. Proc. Natl. Acad. Sci. U.S.A. 99:15908-15913.

Worst, D. J., Gerrits, M. M., Vandenbroucke-Grauls, C. M. J. E., and Kusters, J. G. 1998. *Helicobacter pylori ribBA*-mediated riboflavin production is involved in iron acquisition. J. Bacteriol. 180:1473-1479.

Yang, G., Bhuvaneswari, T. V., Joseph, C. M., King, M. D., and Phillips, D. A. 2002. Roles for riboflavin in the *Sinorhizobium*-alfalfa association. Mol. Plant-Microbe Interact. 15:456-462.

Yurgel, S. N., Rice, J., Domreis, E., Lynch, J., Sa, N., Qamar, Z., Rajamani, S., Gao, M., Roje, S., and Bauer, W. D. 2014. *Sinorhizobium meliloti* flavin secretion and bacteria-host interaction: Role of the bifunctional RibBA protein. Mol. Plant-Microbe Interact. 27:437-445.

Zhang, M., Gao, C., Guo, X., Guo, S., Kang, Z., Xiao, D., Yan, J., Tao, F., Zhang, W., Dong, W., Liu, P., Yang, C., Ma, C., and Xu, P. 2018. Increased glutarate production by blocking the glutaryl-CoA dehydrogenation pathway and a catabolic pathway involving L-2-hydroxyglutarate. Nat. Commun. 9:2114.